JOURNAL OF MATERIALS SCIENCE 15 (1980) 2816–2822

Theory of inclusion controlled grain growth

N. A. HAROUN
College of Engineering, King Abdul-Aziz University, P.O. Box 1540, Jeddah, Saudi Arabia

Different inclusion/grain boundary interactions have been analysed with emphasis on the grain boundary structure and the geometry of the inclusion/boundary profiles. Crystalline inclusions can inhibit grain growth, provided one or more inclusions intersect each boundary. An equation for the limiting grain size, in terms of the volume fraction and the particle size distribution of the inclusions, is derived and is shown to explain the inclusion controlled limiting grain sizes in calcium fluoride and in alumina, as well as grain coarsening in steel. Conditions for the drag of amorphous particles or pores, and for pore isolation are discussed.

1. Introduction

Second phase inclusions can affect the geometry of grain boundary migration, kinetics of grain growth and the ultimate grain size. Depending on the nature of inclusions and the driving force, an inclusion can pin or be dragged or by-passed by grain boundaries [1].

2. Pinning of grainboundaries – earlier theories

Inclusions of a second phase are known to halt or retard grain boundary migration [1]. The effectiveness of inclusions depends on their size and number. For a volume fraction, f, of inclusions whose average particle size is d, a relation has been developed by Zener for the limiting grain size D_1 [2]

$$D_1 = \frac{2d}{3f}. \tag{1}$$

The Zener concept is based on two main assumptions: (i) that a migrating grain boundary does work as one unit, much the same as a curved soap bubble boundary, (ii) that an inclusion exerts a drag along the grain boundary meeting an inclusion at an angle θ (Fig. 1) given by $d\gamma \cos\theta \sin\theta$, where γ is the specific surface energy.

A balance of forces would determine the limiting grain size. Multiplying the drag by the number of inclusions per unit area, and equating to the driving force per unit area led to Equation 1. However, the present author has pointed out that the measured grain boundary curvatures are at least an order of magnitude less than the grain size [3]. This should change the constant in Equation 1 to ~ 0.08 so that

$$D_1 = 0.08\frac{d}{f}. \tag{2}$$

A more serious drawback of the same equation has been shown to be that it does not guarantee that, at the limiting grain size, every boundary meets (and is pinned by) at least one inclusion. The latter condition can be satisfied by the relation [3, 4]

$$D_1 = \frac{1.03d}{f^{1/2}}. \tag{3}$$

The inclusions were assumed uniform in size, d. It was concluded [3, 4] that the limiting grain size would be determined either by the modified Equation 2 for f in the range 0.5% volume or otherwise by Equation 3.

Gladman [5] has considered in detail the profile of a grain boundary around an inclusion to compute the energy changes during unpinning. Considering a two dimensional model of tetrakaidecahedral grains, an equation of the form

$$d_{cr} = \frac{3Df}{\pi}\left(\frac{3}{2} - \frac{2}{Z}\right)^{-1} \tag{4}$$

has been derived. Z is the ratio between a growing grain size diameter and the matrix grain size, assuming that only grains with Z ratio $\geqslant 1.33$ can grow, similar to the earlier Hillert grain growth

0022–2461/80/112816–07$02.70/0 © *1980 Chapman and Hall Ltd.*

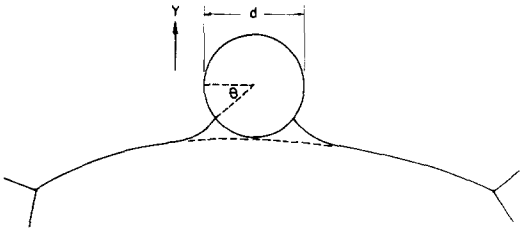

Figure 1 Geometry of inclusion/boundary interaction.

theory [6]. It was proposed that there is a critical inclusion size d_{cr} below which inclusions are ineffective for pinning and above which are insufficient in number to do so. This was used to explain grain coarsening behaviour in austinitic steels containing aluminium nitride inclusions.

3. Mechanism of grain boundary migration

Grain boundary migration can be viewed either through a thermodynamic or an atomistic approach. Typical of the former are Burke and Turnbull's single process theory [7] and Mott's group-theory [8], where all the atoms of a grain boundary have an equal chance to migrate from a convex to a concave grain boundary. The rate is governed mainly by the activation energy and entropy. The interaction of an inclusion with a grain boundary should be considered from an atomistic view.

Earlier models considered grain boundaries as an amorphous region, islands of good fit and bad fit [8] and dislocations [9, 10]. More recently, Gleiter has shown that both high angle [11] and low angle [12] grain boundaries can be viewed as a series of steps of a zig-zag form, made of close packed planes as they meet a boundary. This was based on transmission electron microscopy of an Al–0.39 wt % Cu foil, where patterns of grain boundary lines were observed. Geometrical properties of these lines proved them to be neither ΔS fringes, Moiré fringes nor dislocations [13]. The observations that these lines are displaced on meeting either the foil surface or the thickness fringes together with the occurence of spirals (similar to crystal growth spirals) has confirmed that these lines were interpenetrating steps composed of {1 1 1} planes. The sources of these lines were observed to be grain boundary junctions or screw dislocations. Steps could be observed in 80% of the boundaries, their absence in others could be attributed to electron microscopy resolution limitations.

The concept of coincidence lattice site boundaries i.e. Kronberg–Wilson special angle boundaries [14] was extended using field ion microscopic observations [15, 16] to view the boundary in terms of lattice coincidence [17–19]. Deviation from ideal coincidence is taken by step or ledge formation and superimposed dislocations – the so-called CLD model [20]. Coincidence and twin boundaries would contain no steps. Calculations of the minimum energy configurations in a plane normal to a tilt boundary [21] and in a symmetric tilt boundary [22] led to the same picture for the boundary structure. Coincidence boundaries were observed in ionic compounds e.g. MgO and CdO [23]. It was proposed that nonmetallic crystals would exhibit steps with relatively large dislocation vectors [11]. The step model was shown to be in harmony with many phenomena such as anisotropy of diffusion, grain boundary mobility and energy data [18].

Atoms in a grain boundary could thus be divided as grain atoms that lie in the lattice of either grain or boundary atoms, in the region between two grains: an echo of the old good and bad fit model [8]. Grain boundary migration would thus consist of the emission of atoms from the steps of the shrinking [24] grain to the grain boundary, followed by adsorption on the growing grain. This occurs in stages; namely emission of atoms (and absorption of vacancies) from kinks in the steps to a general step position, diffusion along the step, dissociation from the step into a grain surface position, desorption to grain boundary atoms and finally condensation to a step kink position in the growing grain surface [24]. Analysis of the kinetics of these steps has led to an equation in which the mobility of a grain boundary mainly depends on the step and kink density on both surfaces of the mating grains i.e. on grain boundary orientation [24, 25]. Only for small angle boundary migration is migration carried out by diffusion along dislocation cores [10, 25].

4. Grain boundary – inclusion pinning interaction

Instead of viewing the grain boundary as a flexible membrane the local environment (few atomic layers) around an inclusion should be considered. Surface energy equilibrium necessitates that a boundary should subtend equal angles with both grain inclusion surfaces. The configuration of a migrating curved boundary moving past an inclusion

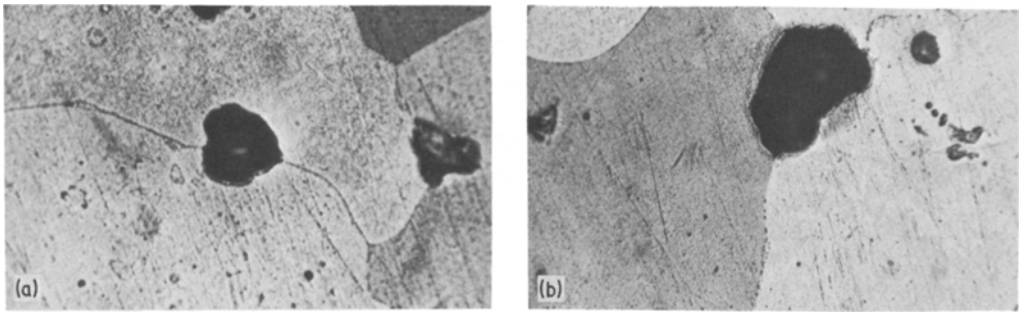

Figure 2 Oxide inclusions in copper (× 115).

should change to a doubly curved profile that ends with a short rather flat portion, as shown in Fig. 1. Typical examples of this profile can be observed around oxide inclusions in copper [16] in Fig. 2, as well as AlN and NbC inclusions in steel [5, 27], and ThO_2 inclusions in tungsten [28].

Adopting the step mechanism of Gleiter [24] the short relatively flat regions near an inclusion should have a less step density, and hence less mobility than others. An additional retarding factor is the possible existence of a gradient of inclusion solute atoms.

Referring to Fig. 1, although the boundary as a whole tends to migrate in the Y-direction, the oppositely curved area in the vicinity of an inclusion would tend to migrate in the opposite direction. The assumption that any group of atoms should tend to migrate according to their own environment, and the necessity of maintaining boundary continuity should bring the migrating boundary to a halt.

5. Criteria for the overall pinning of grain boundaries by inclusions

Following Heuer [29], the driving force for grain boundary migration is taken as $\gamma\Omega/R$, Ω is the atomic volume and R the radius of curvature. According to curvature measurements made in MgO specimens [3] $R \simeq 9D$ i.e. the driving force should be $\gamma\Omega^{2/3}/9D$. The component of the pinning force can be shown to be $\pi d\gamma \cos\theta \sin\theta$. A grain boundary will be pinned if the latter exceeds the driving force i.e. $Dd \sin 2\theta \geqslant 0.07\Omega^{2/3}$. The maximum pinning force is attained when a boundary moving past an inclusion reaches the position where $\theta = 45°$, at which position the inequality becomes: $dD \geqslant 0.07\Omega^{2/3}$. Considering the relative sizes of d, D and Ω it can be shown that any immobile second phase inclusion would pin that boundary. Earlier electron microprobe observations of alumina microstructures, containing ZnO and NiO inclusions [30] showed that these inclusions invariably lie on grain boundaries and corners. The grain sizes of these specimens were grown from 0.3 μm to 24–34 μm. Not a single observation was made of an inclusion lying in the interior of a grain.

Previously, the condition of one inclusion per boundary has been worked for inclusions of a uniform size (Equation 3). Since we are interested in the number of inclusions, it is realized that the presence of a distribution of particle sizes, which is the more general case, might entail considerable error in the estimate. As an illustration, assume inclusions of average size equal to 5 μm in a material whose grain size is 20 μm. For a volume fraction f of inclusions, the number of inclusions per boundary [4] for uniform sized inclusions would be: $0.247D^2X6f/\pi d^2 = 7.52f$. If 1% of the inclusions have a size of only 0.5 μm, these would contribute: $0.01fX7.52(5/0.5)^2 = 7.52f$, i.e. 100% more inclusions. The presence of 1% of 0.1 μm inclusions would similarly increase the number of inclusions about 2500%. Compared to Equation 3 the limiting grain size would be an order of magnitude less in the former case, and 2–3 orders of magnitude less in the latter case.

Now, if a polycrystalline material of average grain size D contains f volume fraction of crystalline inclusions, and these have a particle size distribution: $x_1, x_2, x_3 \ldots x_n$ of particle sizes $d_1, d_2 \ldots d_n$, it can be shown that the number of inclusions per unit area is $3.82f\Sigma x_i/d_i^2$. For an average boundary area of $0.247D^2$ (tetrakaidecahedron model of grain shapes), at least one inclusion would lie on each boundary if

$$D_1 = \left[\sum\left(\frac{x_i}{d_i^2}\right)f\right]^{-1/2} \qquad (4)$$

TABLE I Limiting grain sizes in CaF_2 (μm)

Addition	D_1 (Experimental)	D_1 (Equation 4)	D_1 (Equations 2 and 3)	D_1 (Equation 1)	D_1 (Experimental)/ D_1 (Equation 4)	Inclusions per boundary	
						Based on $\bar{d}$	Based on psd
1 wt% NiO	24.3	24.7	31.8	302.9	0.99	0.42	1
1 wt% CrO_3	23.4	23.56	43.9	329.5	1.38	0.29	1.17
1 wt% MgO	19.1	28.29	48.2	533.3	0.68	0.07	0.82
1 wt% MnO_2	23.8	37.99	35.9	339.6	0.63	0.23	0.79
1 wt% ZnO	14.6	27.88	26.9	306.7	0.52	0.20	0.72

The choice of the model for grain shape has been shown not to affect the estimation critically [4]. Also, the presence of a distribution of grain sizes would not affect the relation since smaller grains not yet satisfying the condition of one inclusion per boundary would ultimately grow to D_1.

If a count of the number of inclusions per unit area, N, is available, Equation 4 can be put in the more workable form

$$D_1 = 2(N)^{-1/2}. \quad (5)$$

In practice, it is believed that grain growth should stop at a size somewhat lower than D_1 in Equations 4 and 5 i.e. when most but not all grain boundaries are pinned, since the motions of different grain boundaries are interlinked. Also inclusions lying at grain corners should be more effective than others. A lesser number of such inclusions is needed to halt grain growth.

An important corollary is to explain the exaggerated growth frequently observed in the course of heat treating materials containing a minor second phase. It is proposed that the critical stage for starting exaggerated growth should be when the grain size reaches a value around 0.3–0.6 of the limiting size. At this stage, the number of inclusions per boundary should be 0.1–0.4 i.e. some boundaries are inhibited while others can grow. This contrast allows the latter to evolve into exaggerated or runaway grains. This affects both the kinetics of grain growth and the grain size distribution [31, 32].

6. Applications of the theory of pinning

6.1. The limiting grain sizes in CaF_2

Calcium flouride powder* was wet mixed with 1 wt% of either MgO, ZnO, MnO_2, NiO or CrO_3 powder. Pressed compacts were air fired at 1000° C until grain size measurements indicated no further growth. Ceramographic preparations were carried out on silion carbide and gamma alumina abrasives followed by etching in 50% HCl solution. The average grain size was taken as 1.56 the average intercept length [33], for which 300–400 intercepts were used for a measurement. The limiting grain sizes are shown in Table I. The particle size distributions (psd) of the additives, as measured by optical microscopy, are shown in Fig. 3. The estimated number of additive inclusions per boundary at the limiting size are shown also in Table I. For comparison, the theoretically calculated limiting grain sizes according to Equations 1 to 4 are included in Table I. Excellent agreement always exists with Equation 4. It can also be seen that the use of Zener formula leads to gross errors in the estimation of the limiting grain size. Equation 3 gives intermediate values. The latter equation was based on the average rather than the distribution of inclusion sizes. Comparison of the estimated inclusion numbers based on either of these is shown in the last two columns of Table I, which emphasizes the importance of taking the distribution into consideration. The

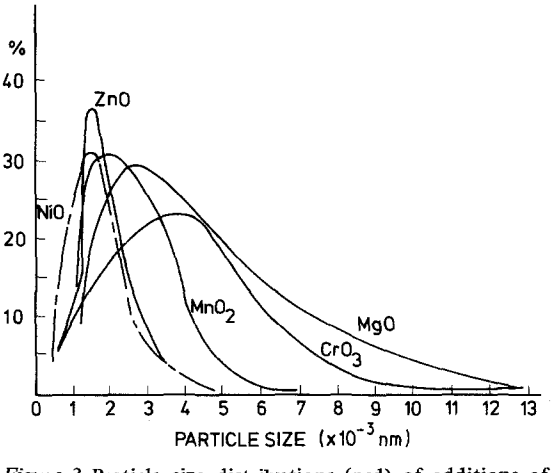

Figure 3 Particle size distributions (psd) of additions of CaF_2.

*Merck W. Germany.

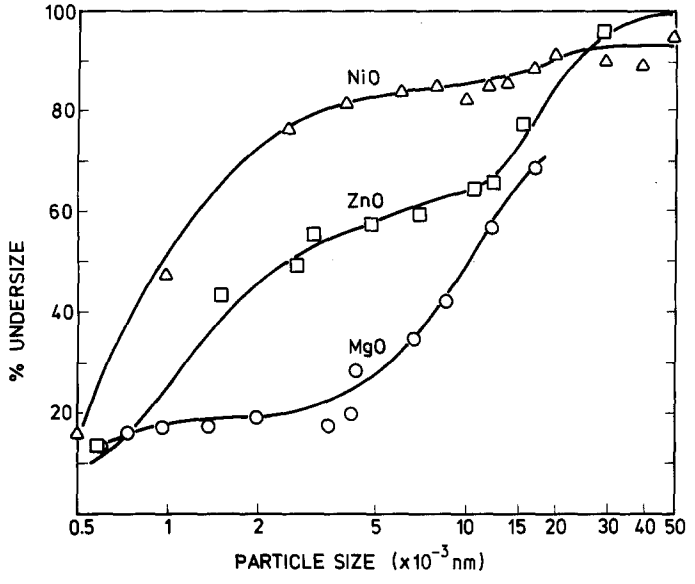

Figure 4 Particle size distributions of additions to Al_2O_3.

small deviations from Equation 4, mostly to the lower side can be readily explained. The microscopic method of particle size determination tends to show the distributions shifted to the larger side due to agglomeration. This is apart from the limitation of the method to sizes above 0.5 μm. Impurity solute drag may contribute to retarding grain growth short of the theoretical D_1. It was pointed out [4] that the condition of one inclusion per boundary is probably over restrictive, as grain growth might practically be brought to a halt once most of the grain boundaries are pinned. Table I shows that at the limiting grain sizes reached, the number of inclusions per boundary ranges between 0.72 and 1.17 which confirms the theory behind Equation 4. The high value of D_1 for CrO_3 inclusions may be due in part to inefficiency of mixing. More probably, the volatility of CrO_3 [34] would remove some of the finest size fractions, that contribute most to the total number of inclusions. Additive respective phase equilibria information for CaF_2 is at present too meagre to elaborate these results any further.

6.2. Limiting grain sizes in alumina

The limiting grain size of Al_2O_3 doped with MgO, NiO or ZnO was shown to depend on the presence of second phase particles on the grain boundaries and corners [30]. Correlation with the amount and particle size of inclusions was sought, based on Equations 2 and 3 [30]. The particle sizes reported were the electron microscopic measurements of the average crystallite sizes, as the NiO and ZnO powders were observed to be loose agglomerates of crystallites [3]. Since the distribution of sizes was shown to be more important for determining the number of inclusions and hence D_1, these will be used to reanalyse the data. The particle size distributions of the three oxide additives are shown in Fig. 4. In Table II a comparison of the limiting grain sizes attained at 1675° C with those predicted by Equations 1, 2, 3 or 4 is made. Again, as with CaF_2, errors of at least two orders of magnitude are incurred if Equation 1 is used, better agreement is achieved with Equations 2 and 3 and excellent agreement is obtained with Equation 4. Deviations from Equation 4 to the higher side can

TABLE II Limiting grain sizes in Al_2O_3 (μm)

Addition	D_1 (Experimental)	D_1 (Equation 4)	D_1 (Equations 2 and 3)	D_1 (Equation 1)	D_1 (Experimental)/ D_1 (Equation 4)	Inclusions per boundary	
						Based on $\bar{d}$	Based on psd
0.25 wt% MgO	43.9	32.40	425.8	3785	1.35	0.01	1.16
0.25 wt% ZnO	33.9	33.31	372.1	3307	1.02	0.01	1.01
0.25 wt% NiO	23.9	25.85	285.5	2529	0.92	0.01	0.96

readily be explained by the vaporization of additive particles [35]. The finer particles (that contribute more to the number of inclusions) should vaporize more readily.

6.3. Grain coarsening in steel

Grain coarsening in steels was observed in the presence of AlN [27] or TiC and NbC [1] inclusions. The grain coarsening temperature was shown to depend on the number of AlN particles [27]. These increase with the AlN content up to 0.8%. Further increases led to agglomeration and hence decrease of the number of AlN particles, that reduced the grain coarsening temperature again [27]. Gladman [27] has estimated a number of 5–6 AlN inclusions per boundary to be the critical number below which grain coarsening is induced. Although these estimates are different from those predicted theoretically above (i.e. 0.1–0.4 inclusions per boundary for the onset of exaggerated growth) the concept of a critical number of inclusions is supported. It can be pointed out that Gladman's estimates were made for coarsening in the temperature range 900 to 1250° C. The morphology of AlN inclusions was acicular (except at 1200° C) for which the estimates of numbers are in doubt.

7. Unpinning of grain boundaries

7.1. Crystalline inclusions in conjunction with other driving forces

The theory of the limiting grain size was based on grain boundary energy as the only driving force for migration. This was equated to the inclusion drag to obtain Equation 4. However, additional driving forces can help a grain boundary to overcome the drag and by-pass an inclusion. One common example of these driving forces is the stored energy of plastic deformation. This is typically 100 times more than the boundary energy driving force [1]. It is known that, in heavily cold worked metals, grain boundaries can migrate against their centre of curvature [28], and hence could be energetic enough to by-pass inclusions. Equation 4 would not hold in these circumstances. Ultrasonic energy accelerated grain growth [36], probably due to by-passing the inclusions in copper [25], is similar to the cold work energy effect.

7.2. Unpinning of pores

Pores can be, and have been shown to be, unpinned from migrating grain boundaries [29]. Unpinning results when the driving force for boundary migration overcomes the pinning force exerted by a second phase. It was shown above that any immobile second phase inclusion lying on a grain boundary can pin that boundary. However, unpinning can occur if pores shrink in such a manner as to be ultimately freed from the boundary. This can be easily visualized as follows. Referring to Figs. 5a and b, a pore lying on a grain boundary or corner and shrinking isotropically would ultimately be unpinned, except for the rare cases of either a 180° or a concentric triple junction, respectively. This is in line with the concept of a critical bubble size for unpinning of gas [37] bubbles. Hence, it is concluded that pores as a second phase can shrink to isolation inside grains and/or be swept by migrating boundaries. The choice of either depends on the relative mobility of pores and grain boundaries.

8. Drag of amorphous inclusions

Liquid and amorphous inclusions can be dragged along with a migrating boundary [38, 39]. This

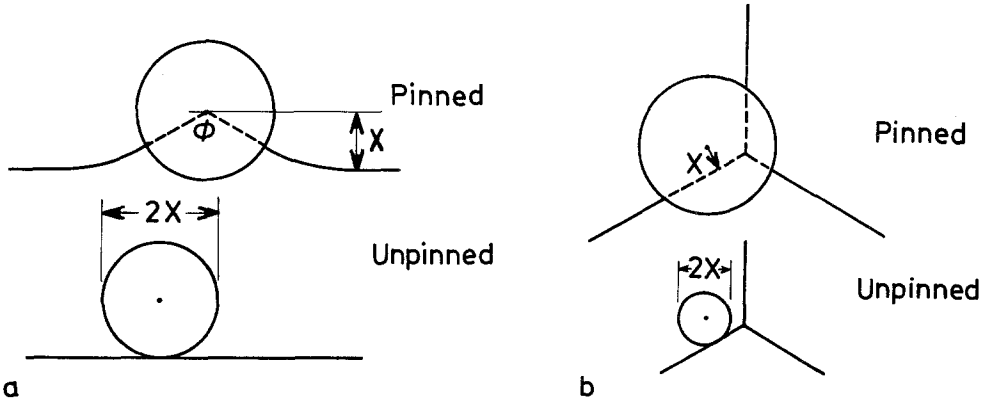

Figure 5 (a) Pore unpinning at a grain boundary, (b) pore unpinning at a grain corner.

has been demonstrated for the drag of amorphous silica inclusions [38, 39] and liquid B_2O_3 and GeO_2 in recrystallized copper [39]. In contrast, no such drag was observed for crystalline Al_2O_3 inclusions [39]. Mobility of inclusions was shown to increase inversely with their viscosity [39]. The process of drag was proposed to be controlled by the diffusion of matrix atoms from the leading to the trailing end of the boundary through the inclusion–matrix interface [39]. Diffusion through the liquid particles can facilitate this process, in contrast to crystalline solids.

A similar mechanism was proposed [25] to explain the observed drag of pores or gas bubbles [37], where surface diffusion will be the dominant process [25]. An alternative mechanism involving prismatic dislocation loops has been proposed [25].

9. Conclusion

Crystalline inclusions can pin grain boundaries when the driving force is surface energy alone. The resulting limiting grain sizes given by Equation 4 are in good agreement with the results of inclusion controlled grain growth in CaF_2 and Al_2O_3. Amorphous solid inclusions and pores can be dragged with migrating boundaries depending on their mobility or viscosity. Pores can also be isolated inside the growing grains, possibly a result of pore shrinkage away rather than being by-passed by the grain boundaries.

References

1. P. COTTERILL and P. R. MOULD, "Recrystallization and Grain growth in Metals" (Surrey University Press, 1976).
2. C. S. SMITH, *Trans. Amer. Inst. Min. Metall. Eng.* **15** (1948) 175.
3. N. A. HAROUN, Ph.D. Thesis, Sheffield University, 1967.
4. N. A. HAROUN and D. W. BUDWORTH, *J. Mater. Sci.* **3** (1968) 326.
5. T. GLADMAN, *Proc. Roy. Soc.* A **294** (1964) 298.
6. M. HILLERT, *Acta Met.* **13** (1965) 227.
7. J. E. BURKE and D. TURNBULL, *Prog. Met. Phys.* **3** (1952) 220.
8. N. F. MOTT, *Proc. Phys. Soc.* **60** (1948) 391.
9. W. T. READ and W. SHOCKLY, *Phys. Rev.* **78** (1950) 275.
10. J. C. M. LI, *J. Appl. Phys.* **32** (1961) 525.
11. H. GLEITER, *Acta Met.* **17** (1969) 565.
12. *Idem., Phil. Mag.* **20** (1969) 821.
13. *Idem., Scripta Met.* **3** (1969) 587.
14. M. L. KRONBERG and F. H. WILSON, *Trans. Amer. Inst. Min. Metall. Eng.* **185** (1949) 501.
15. D. C. BRANDON, B. RALPH, S. RANGANATHAN and M. S. WALD, *Acta Met.* **12** (1964) 813.
16. J. HREN, *ibid.* **13** (1965) 479.
17. D. G. BRANDON, *ibid.* **14** (1966) 1479.
18. K. T. AUST and B. CHALMERS, *Met. Trans.* **1** (1970) 592.
19. F. N. RHINES, *ibid.* (1970) 1105.
20. B. BISHOP and G. A. BUGGEMAN, *J. Mater. Sci.* **7** (1972) 592.
21. M. WEINS, B. CHALMERS, H. GLEITER and M. ASHBY, *Scripta Met.* **3** (1969) 601.
22. M. WEINS, H. GLEITER and B. CHALMERS, *ibid.* **4** (1970) 235.
23. P. CHANDHARI and I. W. MATHEWS, *J. Appl. Phys.* **42** (1971) 3063.
24. H. GLEITER, *Acta Met.* **17** (1969) 853.
25. H. GLEITER and B. CHALMERS, *Prog. Mater. Sci.* **16** (1972) 127.
26. Struers Denmark, Metallographic sample collections, Spec. No. 1100, DIN 1708.
27. T. G. GLADMAN, *Iron Steel Inst. Spec. Rep.* No. 81 (1963) p. 68.
28. J. E. BURKE, "Grain Control in Industrial Metallurgy" (American Society for Metals, Metals Park, Ohio, 1949) p. 1.
29. A. H. HEUER, *J. Amer. Ceram. Soc.* **62** (1979) 317.
30. N. A. HAROUN and D. W. BUDWORTH, *Trans. Brit. Ceram. Soc.* **69** (1970) 73.
31. C. S. SMITH, *Trans. Amer. Inst. Min. Metall. Eng.* **188** (1950) 1021.
32. J. P. NIELSEN, "Recrystallization, Grain growth and Textures" (American Society for Metals, Metals Park, Ohio, 1966) Ch. 4.
33. M. I. MENDELSON, *J. Amer. Ceram. Soc.* **52** (1969) 443.
34. D. B. BINNS, *Trans. Brit. Ceram. Soc.* **77** (1978) 1.
35. M. O. WARMAN and D. W. BUDWORTH, *ibid.* **66** (1967) 253.
36. G. A. HAYES and J. C. SHYNE, *Phil. Mag.* **17** (1968) 859.
37. M. V. SPEIGHT and G. W. GREENWOOD, *ibid.* **9** (1964) 683.
38. M. F. ASHBY and I. G. PALMER, *Acta Met.* **15** (1967) 520.
39. M. F. ASHBY and R. M. A. CANTAMORE, *ibid.* **16** (1968) 1081.

Received 17 December 1979 and accepted 25 April 1980.